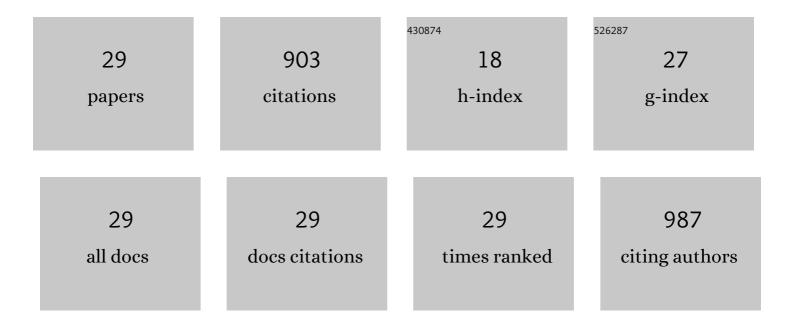
Huizeng Liu

List of Publications by Year in descending order

Source: https://exaly.com/author-pdf/6711282/publications.pdf Version: 2024-02-01



#	Article	IF	CITATIONS
1	Evaluation of Ocean Color Atmospheric Correction Methods for Sentinel-3 OLCI Using Global Automatic <i>In Situ</i> Observations. IEEE Transactions on Geoscience and Remote Sensing, 2022, 60, 1-19.	6.3	8
2	Characteristics and trends of hillside urbanization in China from 2007 to 2017. Habitat International, 2022, 120, 102502.	5.8	9
3	A Glimpse of Ocean Color Remote Sensing From Moon-Based Earth Observations. IEEE Transactions on Geoscience and Remote Sensing, 2022, 60, 1-11.	6.3	2
4	Improving satellite retrieval of oceanic particulate organic carbon concentrations using machine learning methods. Remote Sensing of Environment, 2021, 256, 112316.	11.0	49
5	Estimating ultraviolet reflectance from visible bands in ocean colour remote sensing. Remote Sensing of Environment, 2021, 258, 112404.	11.0	12
6	Digital mapping of zinc in urban topsoil using multisource geospatial data and random forest. Science of the Total Environment, 2021, 792, 148455.	8.0	28
7	Comparing hillside urbanizations of Beijing-Tianjin-Hebei, Yangtze River Delta and Guangdong–Hong Kong–Macau greater Bay area urban agglomerations in China. International Journal of Applied Earth Observation and Geoinformation, 2021, 102, 102460.	2.8	10
8	Use of a multiscalar GRACE-based standardized terrestrial water storage index for assessing global hydrological droughts. Journal of Hydrology, 2021, 603, 126871.	5.4	18
9	Rapid Urbanization Induced Extensive Forest Loss to Urban Land in the Guangdong-Hong Kong-Macao Greater Bay Area, China. Chinese Geographical Science, 2021, 31, 93-108.	3.0	28
10	A Four-Step Method for Estimating Suspended Particle Size Based on In Situ Comprehensive Observations in the Pearl River Estuary in China. Remote Sensing, 2021, 13, 5172.	4.0	5
11	Small water bodies mapped from Sentinel-2 MSI (MultiSpectral Imager) imagery with higher accuracy. International Journal of Remote Sensing, 2020, 41, 7912-7930.	2.9	26
12	Rapid urbanization and policy variation greatly drive ecological quality evolution in Guangdong-Hong Kong-Macau Greater Bay Area of China: A remote sensing perspective. Ecological Indicators, 2020, 115, 106373.	6.3	94
13	High-Frequency Variations in Pearl River Plume Observed by Soil Moisture Active Passive Sea Surface Salinity. Remote Sensing, 2020, 12, 563.	4.0	5
14	Detecting Spatiotemporal Features and Rationalities of Urban Expansions within the Guangdong–Hong Kong–Macau Greater Bay Area of China from 1987 to 2017 Using Time-Series Landsat Images and Socioeconomic Data. Remote Sensing, 2019, 11, 2215.	4.0	33
15	Determining switching threshold for NIR-SWIR combined atmospheric correction algorithm of ocean color remote sensing. ISPRS Journal of Photogrammetry and Remote Sensing, 2019, 153, 59-73.	11.1	25
16	Revisiting effectiveness of turbidity index for the switching scheme of NIR-SWIR combined ocean color atmospheric correction algorithm. International Journal of Applied Earth Observation and Geoinformation, 2019, 76, 1-9.	2.8	9
17	Adaptation and Validation of the Swire Algorithm for Sentinel-3 Over Complex Waters of Pearl River Estuary. , 2018, , .		1
18	Comparison of Machine Learning Techniques in Inferring Phytoplankton Size Classes. Remote Sensing, 2018, 10, 191.	4.0	44

Huizeng Liu

#	Article	IF	CITATIONS
19	Comparison of Satellite-Derived Phytoplankton Size Classes Using In-Situ Measurements in the South China Sea. Remote Sensing, 2018, 10, 526.	4.0	18
20	Spectroscopic Diagnosis of Arsenic Contamination in Agricultural Soils. Sensors, 2017, 17, 1036.	3.8	20
21	Application of Sentinel 2 MSI Images to Retrieve Suspended Particulate Matter Concentrations in Poyang Lake. Remote Sensing, 2017, 9, 761.	4.0	107
22	Improving Spectral Estimation of Soil Organic Carbon Content through Semi-Supervised Regression. Remote Sensing, 2017, 9, 29.	4.0	23
23	Estimating orthophosphate phosphorus concentration in Shenzhen Bay with remote sensing and legacy in-situ measurements. , 2016, , .		1
24	Successive projections algorithm-based three-band vegetation index for foliar phosphorus estimation. Ecological Indicators, 2016, 67, 12-20.	6.3	27
25	New spectral metrics for mangrove forest identification. Remote Sensing Letters, 2016, 7, 885-894.	1.4	49
26	Estimation of arsenic in agricultural soils using hyperspectral vegetation indices of rice. Journal of Hazardous Materials, 2016, 308, 243-252.	12.4	84
27	Estimating leaf nitrogen concentration in heterogeneous crop plants from hyperspectral reflectance. International Journal of Remote Sensing, 2015, 36, 4652-4667.	2.9	29
28	Monitoring Arsenic Contamination in Agricultural Soils with Reflectance Spectroscopy of Rice Plants. Environmental Science & Technology, 2014, 48, 6264-6272.	10.0	83
29	Soil Organic Carbon Content Estimation with Laboratory-Based Visible–Near-Infrared Reflectance Spectroscopy: Feature Selection. Applied Spectroscopy, 2014, 68, 831-837.	2.2	56